JOURNAL OF AGRICULTURAL AND FOOD CHEMISTRY

ARTICLE

pubs.acs.org/JAFC

Physicochemical and Structural Properties of Maize and Potato Starches as a Function of Granule Size

Sushil Dhital, Ashok K. Shrestha, Jovin Hasjim, and Michael J. Gidley*

Centre for Nutrition and Food Sciences, Queensland Alliance for Agriculture and Food Innovation, The University of Queensland, St. Lucia, Brisbane, Queensland 4072, Australia

ABSTRACT: Chemical composition, molecular structure and organization, and thermal and pasting properties of maize and potato starches fractionated on the basis of granule size were investigated to understand heterogeneity within granule populations. For both starches, lipid, protein, and mineral contents decreased and apparent amylose contents increased with granule size. Fully branched (whole) and debranched molecular size distributions in maize starch fractions were invariant with granule size. Higher amylose contents and amylopectin hydrodynamic sizes were found for larger potato starch granules, although debranched molecular size distributions did not vary. Larger granules had higher degrees of crystallinity and greater amounts of double and single helical structures. Systematic differences in pasting and thermal properties were observed with granule size. Results suggest that branch length distributions in both amylose and amylopectin fractions are under tighter biosynthetic control in potato starch than either molecular size or amylose/amylopectin ratio, whereas all three parameters are controlled during the biosynthesis of maize starch.

KEYWORDS: starch granule, heterogeneity, size fractionation, molecular size distribution, crystallinity, helix content

INTRODUCTION

Starch is synthesized by plants in granular form with a wide range of sizes (<1−100 μm in diameter) and shapes (spherical, lenticular, polyhedral, irregular, etc.), characteristic of the botanical origin.[1] Wheat, barley, rye, and triticale starches have a bimodal granule-size distribution consisting of large disk-shaped granules (A-type granules) and small spherical granules (B-type granules), which are readily separated.[2] These A- and B-type granules have different chemical compositions (lipid, protein, and minerals), functional properties (enzymatic digestion, pasting, and thermal), and molecular structures (amylose content and amylopectin branch lengths).[3−6] The amylopectin molecules of the A-type granules consist of a slightly larger amount of long chains that extend through two clusters and a lesser amount of shorter chains that are confined to a single cluster compared with the amylopectin molecules of B-type granules.[2,7]

Maize and potato starch granules have a unimodal size distribution, covering a wide range of granule sizes (particularly for potato), most likely due to the termination of starch granule synthesis at different growth stages. The small granules have been postulated as the immature granules that are unable to completely develop into full-size granules, whereas the large granules are suggested to be the fully developed granules.[8,9] In maize starch, smaller granules reflect the characteristics of unfractionated starch isolated from whole endosperms earlier in kernel development, supporting the hypothesis that these small granules were derived from physiologically younger cells.[10] On top of this, there is a gradient in endosperm cell development in maize starch; for example, the youngest endosperm cell (thus smaller granules) is positioned in the peripheral part of the endosperm.[11,12] Study of the physicochemical properties of starch granules fractionated on the basis of differences in granule size can provide insights into the role that granule size plays in determining structural and functional properties of starches as well as identifying relationships among structural features at different length scales as a function of granule maturity.

Compared with the bimodal size distribution starches, only limited studies have been reported on the physicochemical properties of granule-size-fractionated unimodal starches, particularly maize. This might be due to the practical difficulty of separating maize starch granules, which have a narrow granule-size distribution (2−30 μm). Some differences in physicochemical properties between starch granules of different sizes have been observed previously for both maize and potato starches. Larger maize starch granules contain more amylose than smaller granules.[8,13,14] Similarly, the larger granules of potato starch also have significantly higher amounts of amylose along with lower amounts of proteins and minerals than their smaller counterparts.[15,16] Pasting properties differ for potato starches of different granule size, with the smaller granules showing lower peak, trough, and final viscosities than the larger granules.[17] The gelatinization temperature of the smaller granules of potato starch was significantly higher than that of the larger granules.[18] On the molecular level, the branch chain length distributions of amylopectins from potato starch have been reported to be similar for granules of different sizes.[15]

In a previous study, we successfully applied Stokes' law of sedimentation to separate maize and potato starch granules into predictable size fractions and conducted a comparative study on the amylase digestibility of these fractions.[19] The results showed that the relative accessible surface area of starch granules was the major determinant for amylase diffusivity into starch granules. In this study, we analyze the chemical composition, molecular structure, supramolecular structure (crystallinity and double and single helices), and thermal and pasting properties of granule fractions of maize and potato starches. The use of a greater

Received: June 10, 2011
Revised: August 6, 2011
Accepted: August 14, 2011
Published: August 15, 2011

Table 1. Chemical Composition of Native and Granule-Size-Fractionated Maize and Potato Starches[a]

fraction	rel yield[b] (%)	av size[b] (μm)	lipid (% db)	protein (% db)	ash (% db)	amylose (% db)
MS		13.6	0.79 (0.05) b	0.42 (0.01) b	0.09 (0.01) ab	27.6 (1.81) ab
MS-VS	17.2	9.2	0.96 (0.08) c	0.46 (0.01) b	0.12 (0.02) a	26.0 (1.46) a
MS-S	31.4	13.6	0.76 (0.08) b	0.31 (0.01) a	0.08 (0.03) ab	28.9 (0.62) bc
MS-M	40.6	16.5	0.67 (0.19) b	0.31 (0.01) a	0.07 (0.01) b	29.5 (1.46) bc
MS-L	10.8	20.3	0.33 (0.06) a	0.27 (0.05) a	0.07 (0.01) b	30.1 (0.62) c
LSD[c]			0.27	0.06	0.05	2.0
PS		30.4	0.13 (0.02) xy	0.08 (0.00) x	0.16 (0.06) x–z	36.7 (1.6) x
PS-VS	12.2	15.9	0.20 (0.03) y	0.09 (0.00) x	0.25 (0.01) x	33.8 (0.5) y
PS-S	26.4	28.1	0.16 (0.04) xy	0.03 (0.01) y	0.21 (0.04) xy	35.4 (1.0) xy
PS-M	32.5	40.2	0.13 (0.09) xy	0.02 (0.01) y	0.15 (0.01) yz	36.5 (0.5) x
PS-L	19.8	50.5	0.10 (0.03) xy	0.02 (0.00) y	0.13 (0.04) yz	37.0 (2.1) xz
PS-VL	9.1	67.5	0.06 (0.04) x	0.03 (0.01) y	0.11 (0.02) z	38.8 (1.2) z
LSD[b]			0.11	0.01	0.09	1.9

[a] Different letters in the same column (for lipid, protein, ash, and apparent amylose contents) indicate significant difference at $p \leq 0.05$. Numbers in parentheses are standard deviations. [b] Cited from Dhital et al.[19]. [c] LSD, least significant difference.

number of granule-size fractions (four for maize and five for potato) and a wider range of physicochemical probes than in any previous studies[8,13−18] of granule-size effects allows a more detailed mechanistic understanding of granule-size effects than has so far been reported. In addition to testing specific structure−function hypotheses, a correlation matrix was generated to elicit relationships among the physicochemical properties of starch granule size fractions to further understand the nature and consequences of heterogeneity within native maize and potato starch granules.

MATERIALS AND METHODS

Potato starch (PS, S4251) was purchased from Sigma-Aldrich, Castle Hill, NSW, Australia, and maize starch (MS) was purchased from Penford Australia Ltd., Lane Cove, NSW, Australia. Both starches were fractionated by a repeating sedimentation process as described previously[19] using Stokes' law of sedimentation to predict the sedimentation time for desired granule size. The surface-weighted mean diameters of separated granules were previously determined using a Malvern Mastersizer Hydro 2000MU (Malvern Instruments Ltd., Malvern, U.K.) as described previously.[19] MS granules were separated into very small (MS-VS), small (MS-S), medium (MS-M), and large (MS-L) fractions with surface-weighted mean diameters of 9.2, 13.6, 16.5, and 20.3 μm, respectively (Table 1). Similarly, PS granules were separated into very small (PS-VS), small (PS-S), medium (PS-M), large (PS-L), and very large (PS-VL) fractions with surface-weighted mean diameters of 15.9, 28.1, 40.2, 50.5, and 67.5 μm, respectively (Table 1). The native (unfractionated) MS and PS had mean diameters of 13.6 and 30.4 μm, respectively. The relative yield of the separated starch granules is summarized in Table 1. The moisture contents of all starch samples were adjusted via vapor phase isopiestic equilibration over saturated K_2CO_3 salt solution at 20 °C for 1 week, providing an environment with a relative humidity of 44% to minimize the effect of moisture variation. The resulting moisture content was in the range of 9−11% for all conditioned starch samples as determined by vacuum oven drying overnight at 100 °C.

Lipid contents of starch samples were determined by an acid hydrolysis method.[20] Protein contents (6.25 × N) were determined using a LECO CNS 2000 autoanalyzer (LECO Corp., St. Joseph, MI) following the method of Jung et al.[21] Apparent amylose contents were determined using an iodine colorimetric method[22] without prior defatting of starch samples using Sigma A-0512 and S-9679 as amylose and amylopectin calibration standards, respectively. Mineral contents were determined by dry ashing at 550 °C.[23] Mineral compositions of starch samples were analyzed by inductively coupled plasma optical emission spectrometry (Vista Pro ICP-OES, Varian Pty. Ltd., Mulgrave, VIC, Australia) at spectral wavelengths of 422, 327, 238, 766, 279, 257, 588, 213, and 181 nm for calcium, copper, iron, potassium, magnesium, manganese, sodium, phosphorus, and sulfur, respectively.

The size distributions of fully branched (whole) and debranched molecules in the native and granule-size-fractionated starches were analyzed using a size exclusion chromatography (SEC) system (Agilent 1100 Series SEC system, Agilent Technologies, Waldbronn, Germany) equipped with a refractive index detector (PN3140, PostNova Analytics, Landsberg, Germany) following the methods of Cave et al.[24] and Dhital et al.[25] for fully branched (whole) and debranched molecules, respectively. The hydrodynamic radius (R_h) was converted from the SEC elution volume following the method of Cave et al.[24] using a series of pullulan standards (Polymer Standard Services, Mainz, Germany) with molecular weights (M_p) ranging from 342 to 2.35 × 10^6 Da. The R_h of the pullulan standards was calculated from the molecular weight (M_n) using the Mark−Houwink equation, $V_h = 2KM_n^{(1+\alpha)}/5N_A$, with $V_h = {}^4/_3\,\pi\,R_h^3$, N_A is Avogadro's constant, and the K and α values for pullulan in DMSO with 0.5% w/w LiBr are 2.427 × 10^{-4} dL g^{-1} and 0.6804, respectively. The mass recovery after SEC is essentially 100% within experimental error as reported by Tizzotti et al.,[26] who used the same SEC setup and conditions as used in the present experiments. SEC separates molecules by hydrodynamic size, not by molecular weight. Although there is a unique relationship between hydrodynamic size and molecular weight for linear polymers, that is, the Mark−Houwink equation, there is no such relationship for highly branched molecules, including starch. Hence, the molecular size distributions of fully branched and debranched starch molecules were plotted as SEC weight distribution, w (log V_h), against the logarithm of hydrodynamic radius (log R_h/nm).

X-ray diffraction (XRD) analysis was performed using an X-ray diffractometer (D8 Advance, Bruker AXS GmbH, Karlsruhe, Germany) operating at 40 kV and 30 mA with Cu Kα1 radiation (λ) at 0.15405 nm. The scanning region was set from 3 to 40° of the diffraction angle 2θ, which covers all of the significant diffraction peaks of starch crystallites. A step interval of 0.02° and a scan rate of 0.5°/min were employed for all samples. Crystallinity was calculated as the ratio of the total peak area to the total diffraction area.[27] The diffractograms were smoothed by 13 points using Traces software (version 3.01, Diffraction Technology Pty

Table 2. Mineral Compositions of Native and Granule-Size-Fractionated Maize and Potato Starches[a]

fraction	calcium (ppm)	copper (ppm)	iron (ppm)	potassium (ppm)	magnesium (ppm)	manganese (ppm)	sodium (ppm)	phosphorus (ppm)	sulfur (ppm)
MS	54.9 (12.59) a	1.1 (0.17) ab	1.4 (0.38) a	74.0 (16.52) ab	44.8 (4.04) a	0.5 (0.23) a	132.4 (25.58) a	148.0 (16.04) a	52.0 (7.73) ac
MS-VS	57.3 (3.25) a	1.5 (0.33) a	3.5 (0.17) b	88.3 (17.03) a	43.5 (2.36) a	0.9 (0.17) a	137.1 (6.31) a	158.6 (10.08) a	62.6 (14.71) a
MS-S	22.2 (1.64) b	1.0 (0.27) b	1.5 (0.38) a	60.8 (3.60) b	25.5 (1.36) b	0.2 (0.16) b	74.0 (21.25) b	125.9 (5.00) b	36.4 (2.92) b
MS-M	27.5 (0.78) b	0.8 (0.11) b	1.1 (0.40) a	49.8 (5.60) bc	19.0 (1.07) c	0.1 (0.03) b	69.3 (12.42) b	120.4 (6.29) b	37.2 (4.87) bc
MS-L	21.3 (3.21) b	0.8 (0.06) b	0.8 (0.44) a	35.5 (12.00) c	20.4 (0.37) c	0.1 (0.03) b	60.4 (12.65) b	123.6 (6.06) b	38.8 (6.49) abc
LSD[b]	11.0	0.4	0.7	22.3	4.0	0.3	31.1	17.4	15.2
PS	248.0 (2.25) wz	8.4 (2.91) wx	5.1 (0.64)	60.2 (16.90) w	62.8 (4.28) wy	1.31 (0.07) w	37.0 (7.07) w	629.0 (53.65) w	5.9 (2.16) w
PS-VS	409.5 (17.21) x	10.8 (1.00) w	6.5 (0.19)	86.8 (0.39) x	122.1 (11.57) x	1.50 (0.18) x	45.6 (6.13) x	818.8 (11.64) x	8.3 (0.23) w
PS-S	293.1 (1.02) y	5.5 (0.14) wx	4.8 (1.83)	63.7 (4.25) w	74.5 (0.06) w	1.23 (0.00) wz	16.1 (2.03) y	647.3 (0.05) w	8.1 (1.56) w
PS-M	274.6 (23.85) wy	7.9 (4.51) wx	3.0 (0.10)	62.0 (16.03) w	64.6 (0.87) wy	1.09 (0.00) y	16.1 (2.46) y	568.1 (21.73) y	2.6 (0.39) x
PS-L	232.2 (9.44) wz	7.7 (0.62) wx	3.6 (0.31)	59.7 (8.10) w	64.6 (0.77) wy	1.13 (0.06) yz	7.8 (2.01) z	535.8 (3.27) y	2.4 (0.87) x
PS-VL	230.2 (31.09) z	4.9 (0.80) x	4.7 (2.72)	79.9 (10.23) wx	54.2 (5.43) wy	1.16 (0.10) yz	11.2 (1.24) yz	488.2 (24.64) z	1.5 (1.70) x
LSD	43.9	5.5	3.3	22.4	13.4	0.2	7.5	64.0	3.3

[a] Different letters in the same column indicate significant difference at $p \leq 0.05$. Numbers in parentheses are standard deviations. [b] LSD, least significant difference.

Ltd., Mitchell, ACT, Australia) before the percentage of crystallinity was calculated.

Starch samples were analyzed by solid-state ^{13}C nuclear magnetic resonance (NMR) spectroscopy using a Bruker MSL-300 spectrometer (Bruker, Karlsruhe, Germany). Spectral acquisition and interpretation methodology as described elsewhere[28] was used to quantify the double helices, single helices, and amorphous conformational features.

The gelatinization properties of starch samples were analyzed using a differential scanning calorimeter (DSC) (DSC 1, Mettler Toledo, Schwerzenbach, Switzerland). Each sample (~4 mg) was mixed with ~12 mg of deionized water in a DSC pan (aluminum low pressure, 40 μL), which was then hermetically sealed. The pans were held at 10 °C for 5 min and then heated to 120 at 5 °C/min. The onset (T_o), peak (T_p), and conclusion temperatures (T_c) and the enthalpy of gelatinization (ΔH) were determined using the built-in software (STARe System, Mettler Toledo).

Pasting properties of starch samples (8% w/w in distilled deionized water) were analyzed using a Rapid Visco Analyzer (RVA) (Newport Scientific, Warriewood, NSW, Australia) following the method of Dhital et al.[29] Peak viscosity (PV), trough viscosity (TV), final viscosity (FV), and pasting temperature (PT) were determined from the pasting curve using Thermocline version 2.2 software (Newport Scientific).

Results were expressed as means with standard deviations in parentheses from at least duplicate measurements, except for XRD and NMR, for which only single experiments were performed. Analysis of variance (ANOVA) was used to determine the least significance at $p \leq 0.05$ using Genstat 5 (release 3.2, Lawes Agricultural Trust, Harpenden, Hertfordshire, U.K.), and correlation coefficients were determined by using Microsoft Office Excel 2007 (Microsoft Corp., Redmond, WA).

RESULTS AND DISCUSSION

Chemical Composition of Starches. The lipid, protein, amylose, and ash contents of native and granule-size-fractionated MS and PS are presented in Table 1, and specific inorganic element contents are presented in Table 2. MS contained greater amounts of lipids (0.79%) and proteins (0.42%) than PS (0.13 and 0.08%, respectively), consistent with previous results.[30,31] MS lipids are essentially monoacyl lipids (free fatty and lysophospholipids) and are present inside the granules (internal lipids)[32] either independently or as amylose−lipid complexes.[33] On the other hand, the majority of PS lipids are surface lipids[32] probably derived from the amyloplast membrane covering the starch granule. PS had a greater amount of minerals (ash) (0.16%) than MS (0.09%). Phosphorus, calcium, potassium, magnesium, and sodium were the major minerals in both starches. Among them, phosphorus was the most abundant at 629 and 148 ppm in PS and MS, respectively. Cereal starches, such as MS, contain phosphorus mainly in the form of phospholipids, whereas, in PS, phosphorus is bound to the amylopectin molecule as phosphate monoesters.[34] Elevated levels of cations in PS compared with maize starch may be related to the negatively charged phosphate groups. It is also noted that the level of magnesium is greater in the native (unfractionated) starches than in the fractionated starches, suggesting that minerals might be dissolved during the multiple aqueous treatments involved in fractionation.

The proportions of lipids, proteins, and minerals decreased significantly with increasing granule size for both MS and PS (Tables 1 and 2). Noncarbohydrate materials including lipids, proteins, and minerals have been reported to be more concentrated at the surface of starch granules.[35−37] The higher contents of noncarbohydrate materials in smaller granules are therefore attributed to their larger surface area per unit volume compared with larger granules. The apparent amylose, amylose measured in the presence of native lipids, increased with granule size for both MS and PS (Table 1) as previously reported.[8,13,14,17,38] As the types of lipids found in maize and potato are different in nature,[32,33] defatting prior to amylose content analysis by iodine colorimetry using 75% propanol as mentioned in standard protocol[22] might be able to completely remove surface lipids in potato starch granules, but is not likely to remove all internally bound lipids in maize starch granules. Hence, to avoid this inconsistency, the apparent amylose content without prior defatting is deemed to be more appropriate to represent the different starch granule fractions rather than the absolute amylose content after defatting. In the storage organs of maize and potato, the apparent amylose content increases with starch granule size and the radial distance from the hilum.[8,38] This is mainly due to the activity of granule-bound starch synthase

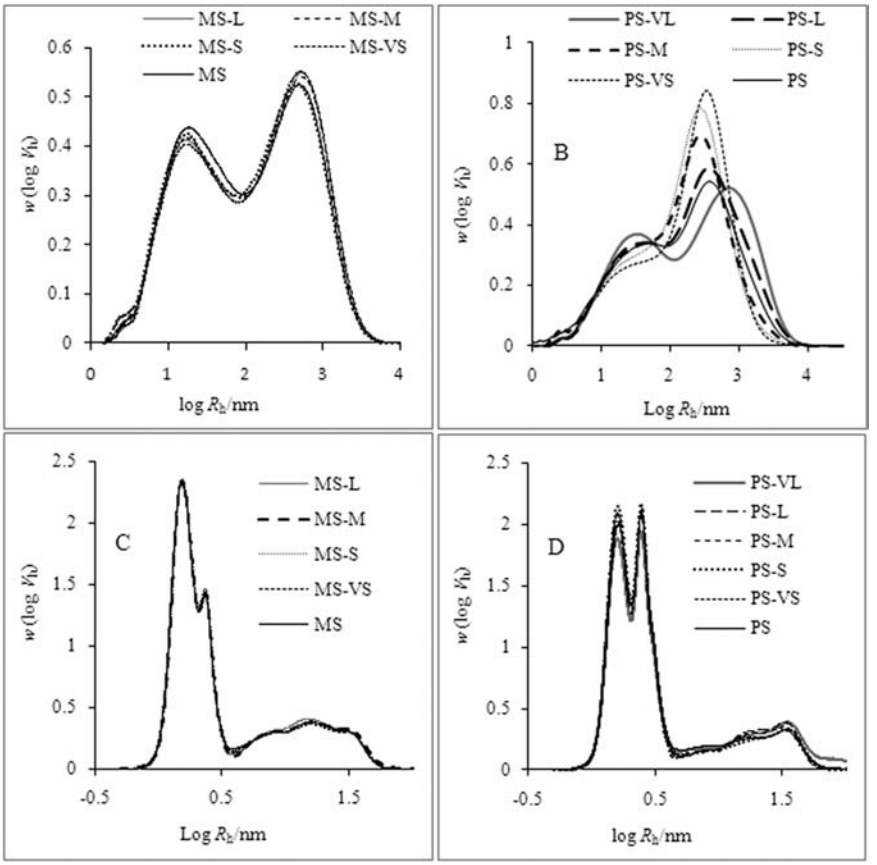

Figure 1. Fully branched size distributions (area normalized) of granule-size-fractionated maize starch (A) and potato starch (B). Debranched size distributions (area normalized) of granule-size-fractionated maize starch (C) and potato starch (D).

(GBSS-I), the enzyme responsible for synthesizing amylose, which is higher at the later stage of starch synthesis.[14,39]

Apparent Size Distribution of Starch Molecules. The size distributions of fully branched molecules (normalized to the total peak areas) of the native and granule-size-fractionated MS and PS showed two well-resolved peaks (R_h < 100 nm and 100–10000 nm) assigned to amylose-rich and amylopectin-rich molecules, respectively (Figure 1A,B). However, the ratio of amylose and amylopectin peaks should not be used to quantify the actual amylose content as there are different specific refractive index increment dn/dc (change in refractive index with polymer concentration) values for amylose and amylopectin in DMSO containing 0.5% w/w LiBr (0.0929 and 0.0717 mL g^{-1}, respectively) and band broadening of SEC peaks causing the overlapping (or incomplete separation) of amylose-rich and amylopectin-rich peaks. Size distributions of fully branched MS fractions were almost similar, although their apparent amylose contents were different (Table 1). This suggests that the lower apparent amylose content in the smaller MS granules is predominantly due to the higher amount of lipids in these granules that might have complexed with amylose and thereby reduces the amount of free amylose available to form a complex with iodine. In contrast, the peak area of amylose and the hydrodynamic size of amylopectin molecules observed from the size distributions of fully branched PS fractions (Figure 1B) increased with increase in granule size. The trend observed in the peak areas of amylose of the PS fractions is in agreement with their apparent amylose contents (Table 1), with the larger granules containing more amylose than the smaller granules. As the lipid content in PS is much lower than that in MS (Table 1), amylose/lipid complexation is not expected to cause a major difference between apparent and true amylose contents for PS.

The size distribution of debranched starches (normalized to the total peak areas) (Figure 1C,D) can be divided into amylopectin branches (R_h < 4 nm) and amylose branches (R_h between 4 and 100 nm). The amylopectin branches can be further divided into two groups: the smaller outer branches that are confined to one lamella (A and B1 chains, R_h < 2 nm) and the longer inner branches that span more than one lamellae (B2, B3, ..., R_h between 2 and 4 nm).[40] In agreement with the size distributions of fully branched starch (Figure 1A), the size distributions of debranched starch of MS fractions (Figure 1C) were almost identical, whereas the size distributions of debranched starch of PS fractions (Figure 1D) showed an increase in the proportion of amylose branches to amylopectin branches with increasing granule size. However, the size distributions of amylopectin branches among the PS fractions (Figure 1D) were almost identical despite the difference in the hydrodynamic size of the fully branched amylopectin from these fractions, which is in agreement with observations reported by Noda et al.[15] Thus, branch chain lengths of amylose and amylopectin do not vary with granule size (for both MS and PS) or the size of fully branched molecules (for PS). This implies a tight biosynthetic control of branch chain lengths for both amylose and amylopectin in maize and potato starches. In contrast, for PS, the whole amylopectin molecular size and the relative proportions

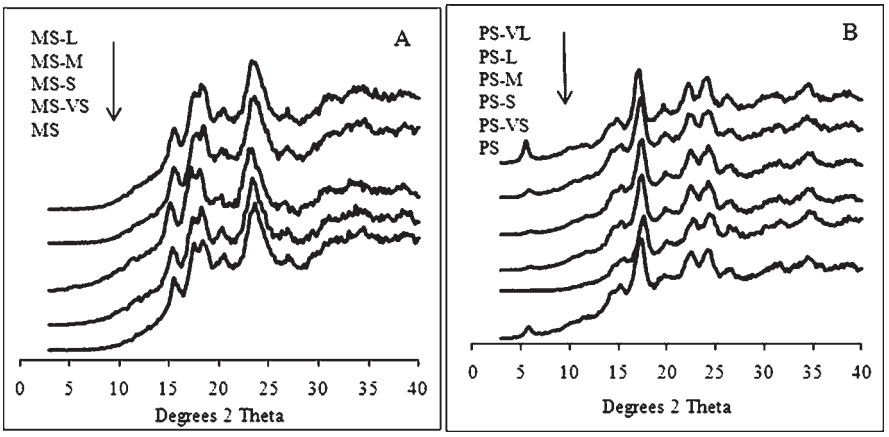

Figure 2. X-ray diffractograms for granule-size-fractionated maize starch (A) and potato starch (B). Direction of arrow denotes the sequence of graphs, starting from top.

Table 3. Crystallinity (Quantified by XRD[a]) and Molecular Order (Measured by NMR[a]) of Native and Granule-Size-Fractionated Maize and Potato Starches

		NMR			
fraction	XRD (crystallinity, %)	V-type polymorph (single helix, %)	double helix (%)	amorphous (%)	noncrystalline double helix[b] (%)
MS	23.5	2.7	28.6	68.6	5.1
MS-VS	22.2	3.5	24.3	72.1	2.1
MS-S	23.3	3.3	25.8	70.8	2.5
MS-M	23.5	2.7	28.5	68.7	5.0
MS-L	24.1	2.4	29.2	68.3	5.1
PS	25.9	1.7	27.2	70.9	1.3
PS-VS	23.2	2.3	26.8	70.8	3.6
PS-S	24.5	2.0	27.2	70.7	2.7
PS-M	25.5	1.6	27.5	70.7	2.0
PS-L	26.1	1.4	28.4	70.1	2.3
PS-VL	28.3	1.1	28.8	70.0	0.5

[a] XRD and NMR calculations are within CV of 5%. [b] Noncrystalline double helix (%) = double helix (%) − crystallinity (%).

of amylose and amylopectin do not appear to be as tightly controlled.

From the combination of branched and debranched distributions, it is evident that there are different reasons for the similar increases of apparent amylose content with granule size for both PS and MS (Table 1). For PS, this is due to a greater proportion of linear and sparsely branched chains with R_h > 4 nm, whereas for MS, neither branched nor debranched molecular size distributions vary with granule size; therefore, the variation of the apparent amylose content with granule size (Table 1) is most likely a reflection of the extent of lipid binding.

Crystallinity and Molecular Order in Starch Granules. The crystalline polymorphs of native starch granules, as revealed by X-ray diffractometry, are classified into A-, B-, and C-type polymorphs. As expected, all MS samples displayed the A-type diffraction pattern with major diffraction peaks at ∼15, 17, 18, and 23° 2θ, and all PS samples had the B-type pattern with major peaks at 17, 22, and 24° 2θ (Figure 2).[41] However, the nonoverlapping peak at 5° 2θ was observed only for larger and unfractionated PS. The relative crystallinity (Table 3) increased with the size of starch granules from 22.2 (MS-VS) to 24.1% (MS-L) and from 23.2 (PS-VS) to 28.3% (PS-VL). The granule size showed a strong positive correlation with relative crystallinity ($R \geq 0.98$, $p \leq 0.05$) for both MS and PS. The crystallinity results agree with qualitative results previously reported for granule-size-fractionated waxy maize, normal maize, and cassava starch.[13,42] The lower crystallinity in smaller granules of MS and PS suggests that molecules closer to the hilum are less able to align into crystallites than those closer to the surface. However, the results from MS suggest that the inability of the molecules closer to hilum to form crystalline structures is not due to differences in branch chain lengths, as these do not vary with granule size.

The X-ray diffractograms did not show any obvious differences among the MS fractions, indicating that the nature of individual crystallites is similar in all MS granules regardless of the granule size. However, for PS, the peak intensity at 5.4° 2θ (Figure 2B) increased markedly with granule size; minor peaks around 15−16° 2θ also appeared to sharpen with increasing granule size, whereas other peaks at higher angles (lower *d*-spacings) did not show such obvious differences. The small granules have been

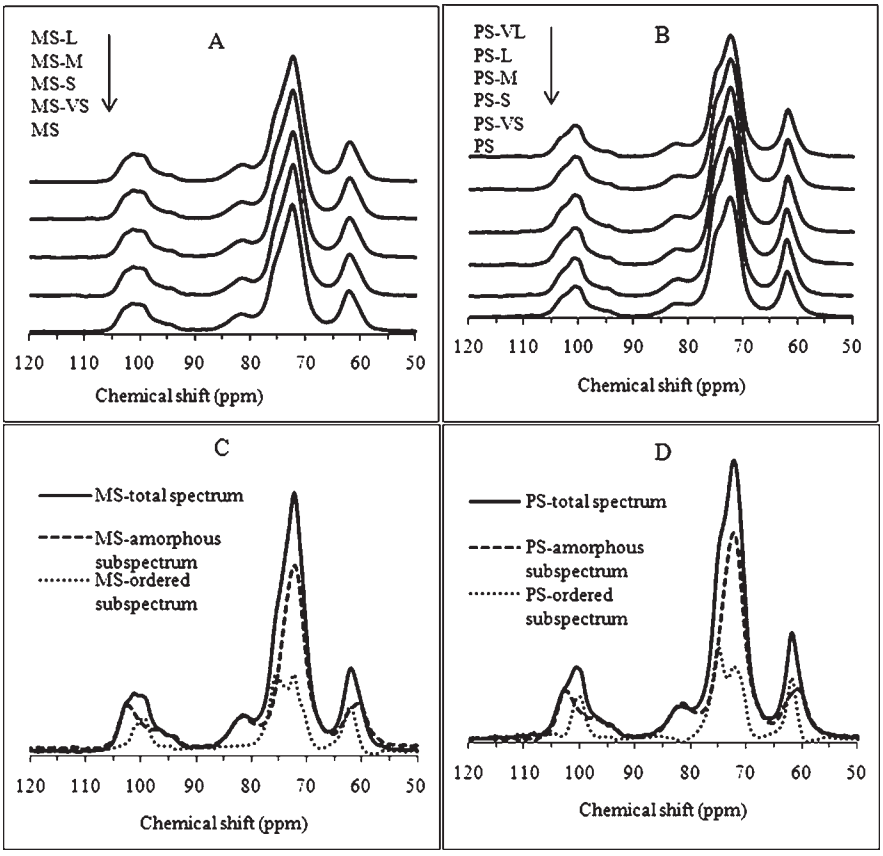

Figure 3. ^{13}C NMR spectra: granule-size-fractionated maize starch (A) and potato starch (B). Separation of ^{13}C NMR spectra into ordered and amorphous subspectra: granule-size fractionated maize starch (C) and potato starch (D). Direction of arrow (in A and B) denotes the sequence of graphs, starting from top.

postulated as those that have not reached full maturity;[8−12] thus, the increase of the peak at 5.4° 2θ with granule size suggests that crystals with larger interplanar spacing (d-spacing) as represented by peaks at lower diffraction angles are developed in the later stage of granule growth. The implication is that crystallinity in potato starches is developed (annealed) slowly during the course of granule deposition.

Panels A and B of Figure 3 show the solid-state ^{13}C NMR spectra of MS and PS size fractions, respectively. The subspectra representing the contributions from amorphous and ordered phases of MS and PS are illustrated in panels C and D of Figure 3, respectively. The results from quantitative analysis of ordered subspectra (by peak fitting to known spectra for double-helical and single-helical polymorphs[28]) are summarized in Table 3. Similar to the relative crystallinity, the amount of double helices increases with increase of granule size for MS and PS. The amount of double helices in MS-VS fraction was 24.3%, ∼5% lower than for the MS-L fraction, whereas only ∼2% difference was observed between PS-VS and PS-VL fractions. The crystalline structure of granular starch is attributed to the regular arrangement of double helices formed by amylopectin branches. However, not all double helices of amylopectin branches are involved in forming crystalline regions, as the amount of double helices is typically greater than the amount of crystallites.[43] This phenomenon was observed in all MS and PS fractions (Table 3). Furthermore, the difference between the amount of double helices and the relative crystallinity in the MS-VS fraction was ∼3% lower than that of the MS-L fractions, whereas that of the PS-VS fraction was ∼3% higher than the PS-VL fraction (Table 3). This suggests that the larger granules of MS have more double helices in the noncrystalline regions, and the opposite is true for larger granules of PS. The decrease in the noncrystalline double-helix content with the increase in granule size for PS (Table 3) shows that the major difference in the diffraction patterns (Figure 2) of PS fractions is due to less perfect alignment of helices rather than different amounts of helices, consistent with steric constraints on helix packing near the hilum.

The percentage of single helices decreased with increasing granule size for MS and PS (Table 3), and the amount of single helices was positively correlated ($R \geq 0.95$, $p \leq 0.05$) with the lipid content, suggesting that lipids in both MS and PS granules participate in single-helical complexes with amylose. However, as a significant negative relationship was obtained in PS between apparent amylose content and single-helix content, the formation of helical complexes appears to be affected by both the content and location of lipid and amylose in the starch granules and is not necessarily related to apparent amylose content. The difference in the amount of single helices among the fractions as observed by NMR (Table 3) did not lead to any distinct difference in the intensity of the peak at 20.2° 2θ (the major peak in the V-type diffraction pattern[41]) in the X-ray diffractograms (Figure 2), indicating that the relatively low levels of single helices in the MS and PS fractions are insufficient to generate V-type crystallinity.

Thermal Properties. Starch gelatinization is a complex phenomenon involving dissociation of amylopectin double helices in

Table 4. Thermal Properties of Native and Granule-Size-Fractionated Maize and Potato Starches[a]

fraction	T_o (°C)	T_p (°C)	T_c (°C)	$T_c - T_o$ (°C)	ΔH (J/g)
MS	64.0 (0.01) a	67.9 (0.01)	71.9 (0.05) a	7.9 (0.06) a	11.4 (0.30)
MS-VS	63.2 (0.05) b	68.5 (0.06)	72.7 (0.06) b	9.5 (0.11) b	10.8 (0.35)
MS-S	64.4 (0.20) c	68.3 (0.16)	72.0 (0.13) a	7.6 (0.06) c	10.8 (0.25)
Ms-M	64.3 (0.25) c	67.8 (0.16)	71.6 (0.13) c	7.3 (0.11) d	11.4 (0.04)
MS-L	64.2 (0.11) c	66.4 (2.06)	71.6 (0.08) c	7.3 (0.04) d	11.4 (0.49)
LSD[b]	0.4	2.3	0.2	0.2	0.8
PS	58.6 (1.03)	63.7(0.37) w	69.3 (0.37) w	10.7 (0.65) w	16.5 (0.59) wy
PS-VS	57.9 (0.16)	63.5 (0.12) w	70.8(0.01) x	14.0 (0.17) x	14.9 (0.13) x
PS-S	58.0 (0.03)	63.0 (0.28) wx	69.7 (0.01) w	12.0 (0.04) y	14.9 (0.57) x
PS-M	57.8 (0.07)	62.9 (0.18) wx	69.2 (0.17) w	11.4 (0.10) yz	15.8 (0.03) y
PS-L	57.6 (0.07)	62.6 (0.11) x	68.4 (0.17) y	10.8 (0.13) wz	15.9 (0.13) yz
PS-VL	57.9 (0.40)	62.2 (0.50) x	68.3 (0.06) y	10.4 (0.17) w	16.7 (0.13) wz
LSD	1.1	0.8	0.4	0.7	0.8

[a] Different letters in the same column indicate significant difference at $p \leq 0.05$. Numbers in parentheses are standard deviations. [b] LSD, least significant difference.

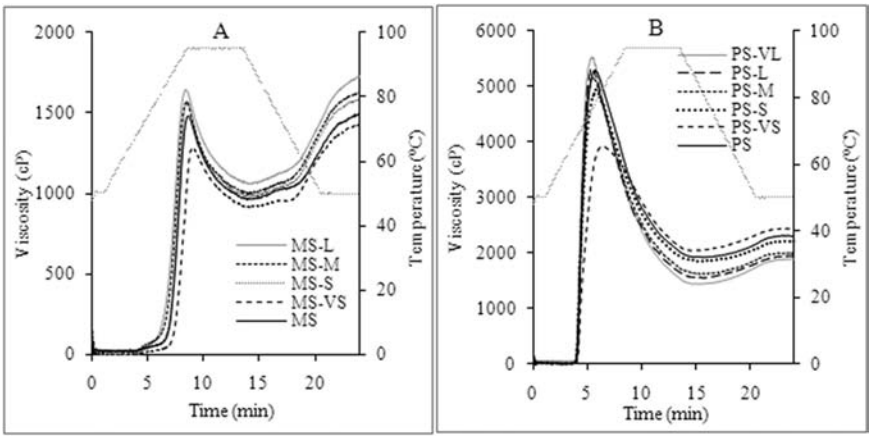

Figure 4. Rapid Visco Analyzer pasting plots of granule-size-fractionated maize starch (A) and potato starch (B). Direction of arrow denotes the sequence of graphs, starting from top.

the crystalline regions of starch granules.[43] The gelatinization properties of granule-size-fractionated MS and PS are summarized in Table 4. T_p and T_c decreased slightly with increasing granule size, whereas T_o was almost constant (apart from the MS-VS fraction). Consequently, the larger granules had a narrower gelatinization temperature range ($\Delta T = T_c - T_o$) than the smaller ones. The ΔH increased from 10.8 to 11.4 J g^{-1} and from 14.9 to 16.7 J g^{1-} with increasing granule size for MS and PS fractions, respectively. The gelatinization temperature reflects the heat stability of the crystalline structure, whereas the ΔH reflects the degree of crystallinity. Although PS has a higher ΔH than MS, it is likely that the higher amount of phosphate monoester in PS causes instability of the starch crystalline structure, thereby lowering the gelatinization temperature. The increase of ΔH in parallel with increases in crystallinity and double-helix content and the decrease in ΔT with increase in granule size for both MS and PS suggest that larger granules have more uniform crystallites than smaller granules,[44] reflecting the smaller relative amount of the less organized hilum in larger granules. An alternative explanation that a greater amount of internal lipids in smaller granules might contribute to lowering endothermic energy and increase in gelatinization peak temperature[5] seems less likely, given the similar DSC property changes (Table 4) but different levels of lipids present (Table 1) in the MS and PS fractions. The variation of ΔH with granule size of PS and MS is in agreement with results reported by Singh and Kaur.[18] However, Utrilla-Cello et al.[14] found the opposite trend, with smaller (MS) granules having higher ΔH values, possibly due to their use of a grinding process to isolate starch from the kernels. During grinding, it is likely that the larger granules will suffer more shear damage than the smaller granules, lowering the ΔH value for larger granules.

Pasting Properties. The pasting curves of native and granule-size-fractionated MS and PS are shown in Figure 4, with parameter values summarized in Table 5. All starch samples displayed shear thinning behaviors, with PS being more shear sensitive than MS. Shear thinning in RVA is observed if the viscosity breakdown ratio (BDR; the ratio of trough to peak viscosity) is lower than unity.[45] The BDR of MS (including size fractions) is almost constant at 0.6, whereas values ranged from 0.2 to 0.5 for PS, decreasing with increase in granule size, larger granules being more shear sensitive than smaller granules in PS.

The relatively high peak viscosity (PV) and low pasting temperature (PT) of PS followed by rapid thinning are attributed to a relatively high concentration of phosphorus (Table 2) as phosphate monoester derivatives on amylopectin branches.[34] The negatively charged phosphate groups cause charge−charge repulsion and reduce the tendency for interchain associations, facilitating the hydration of starch granules during heating. The high PV of highly swollen granules is therefore followed by a subsequent sharp decline in viscosity due to the shear-induced breakdown of these fragile swollen structures. On the other hand, MS contains only a trace amount of phosphate monoester, as most of the phosphorus in MS is in the form of phospholipids.[31,34] Furthermore, the greater amounts of surface lipids and proteins in MS compared with PS (Table 1) restrict granule swelling, unless they are first removed by, for example, sodium dodecyl sulfate extraction.[47] The single-helical complexes between amylose and lipid as suggested by NMR spectral analysis (Table 3) can also retard the swelling of starch granules.[46] Thus, MS showed higher PT and lower PV than PS (Figure 4), even though PS contained less amylopectin, which is responsible for the swelling of starch granules, than MS (Table 1).

Significant differences in the pasting profiles and parameters (PT, PV, TV, and FV) among the starch fractions of different granule sizes, in general, were observed for both PS and MS (Table 5; Figure 4). PV increased significantly with the increase in the granule size of both MS and PS (Table 5), which is in agreement with previously reported results for potato, canna, wheat, triticale, and barley starches.[2,15,17,48] At PV, the rate of granule swelling (and, therefore, the increase in viscosity) is considered to be equal to the rate of breakdown of the granules.[49] During initial swelling, (swollen) granule integrity is largely maintained, and viscosity is mostly due to space-filling effects. In this regime, it is expected that larger swollen granules would be more effective at viscosity generation as they can form intergranular contacts at a lower concentration than smaller swollen granules. An alternative explanation for the effect of granule size on PV can be derived from molecular considerations. The swelling behavior of starch granules is driven by amylopectin at temperatures above that required for melting of crystallites (Table 4); the presence of amylose reduces the concentration of amylopectin, and the presence of amylose−lipid complexes and surfactant-extractable lipid and protein inhibits the swelling of starch granules.[46,47] The increase in PV (Table 5) correlated significantly with the decrease in lipid contents, although the apparent amylose contents were increasing (Table 1), suggesting that PV was affected more by the lipid content than by the apparent amylose content. The higher lipid content associated with amylose−lipid complexes (Table 3) and the higher amount of surface-associated lipid and protein could have inhibited granule swelling and lowered PV to greater extents in smaller granules compared to larger granules of both starches (Table 5). Although significant negative correlation was observed between mineral content and PV, this is very unlikely because the higher

Table 5. Pasting Properties of Native and Granule-Size-Fractionated Maize and Potato Starches[a]

fraction	PT (°C)	PV (cP)	TV (cP)	FV (cP)
MS	83.6 (0.0) a	1463 (28) a	956 (7) a	1475 (25) a
MS-VS	86.1 (0.5) b	1281 (2) b	896 (23) b	1412 (16) b
MS-S	82.8 (0.1) c	1565 (12) c	970 (15) ac	1574 (4) c
MS-M	80.6 (0.2) d	1569 (8) c	990 (12) c	1619 (21) d
MS-L	78.4 (0.2) e	1655 (7) d	1054 (12) d	1727 (7) e
LSD[b]	0.7	37	39	40
PS	66.6 (0.1) u	5272 (21) u	1901 (17) u	2299 (2) u
PS-VS	67.2 (0.1) v	3958 (43) v	2041 (0) v	2444 (6) v
PS-S	66.9 (0.1) uv	4915 (35) w	1888 (49) w	2258 (65) u
PS-M	66.7 (0.0) u	5142 (51) x	1630 (13) x	2011 (12) w
PS-L	67.1 (0.1) v	5328 (2) u	1552 (2) y	1937 (12) x
PS-VL	66.7 (0.2) u	5462 (96) y	1447 (103) z	1904 (4) x
LSD	0.3	124	54	67

[a] Different letters in the same column indicate significant difference at $p \leq 0.05$. Numbers in parentheses are standard deviations. [b] LSD, least significant difference.

Table 6. Pearson's Correlation Matrix of Different Parameters of Granule-Size-Fractionated Maize Starch[a]

parameter	size	lipid	protein	minerals	amylose	PV	TV	FV	PT	ΔH	T_o	T_p	T_e	Crys	SH	DH
size	1															
lipid	−0.97*	1														
protein	−0.9	0.84	1													
minerals	−0.89	0.78	0.97*	1												
amylose	0.93	−0.9	−0.99**	−0.99**	1											
PV	0.92	−0.9	−0.99**	−0.97*	0.99**	1										
TV	0.99**	−0.98*	−0.93	−0.89	0.94*	0.94*	1									
FV	0.99**	−0.96*	−0.95*	−0.92	0.96*	0.96*	0.99**	1								
PT	−0.99**	0.95*	0.92	0.91	−0.95*	−0.93	−0.98*	−0.99**	1							
ΔH	0.9	−0.8	−0.72	−0.78	0.8	0.73	0.84	0.84	−0.91	1						
T_o	0.71	−0.6	−0.93	−0.94*	0.91	0.92	0.75	0.79	−0.74	0.53	1					
T_p	−0.91	0.97*	0.7	0.63	−0.73	−0.73	−0.91	−0.88	0.89	−0.8	−0.41	1				
T_e	−0.93	0.83	0.95*	0.98*	−0.98*	−0.95*	−0.92	−0.94*	0.95*	−0.88	−0.87	0.71	1			
Crys	0.98*	−0.9	−0.97*	−0.95*	0.98*	0.97*	0.98*	0.99**	−0.98*	0.83	0.83	−0.84	−0.96*	1		
SH	−0.97*	0.95*	0.81	0.81	−0.86	−0.82	−0.94*	−0.94*	0.97*	−0.96*	−0.58	0.92	0.89	−0.92	1	
DH	0.97*	−0.9	−0.84	−0.87	0.9	0.85	0.92	0.93	−0.97*	−0.97*	0.66	−0.85	−0.94*	0.93	−0.98*	1

[a] PV, peak viscosity; TV, trough viscosity; FV, final viscosity; PT, pasting temperature; ΔH, gelatinization enthalpy, T_o, onset gelatinization temperature; T_p, peak gelatinization temperature; T_e, end gelatinization temperature; Crys, crystallinity; SH, single helix; DH, double helix. *, significance difference at $p \leq 0.05$; **, significance difference at $p \leq 0.01$.

Table 7. Pearson's Correlation Matrix of Different Parameters of Granule-Size Fractionated Potato Starch[a]

parameter	size	lipid	protein	minerals	amylose	PV	TV	FV	PT	ΔH	T_o	T_p	T_e	Crys	SH	DH
size	1															
lipid	−0.99**	1														
protein	−0.66	0.7	1													
minerals	−0.96**	0.97**	0.78	1												
amylose	0.99**	−0.99**	−0.71	−0.96**	1											
PV	0.89*	−0.91*	−0.93*	−0.93*	0.91*	1										
TV	−0.97**	0.97**	0.76	0.99**	−0.96**	−0.92*	1									
FV	−0.93*	0.97*	0.82	0.99**	−0.93*	−0.94*	0.99**	1								
PT	−0.58	0.59	0.63	0.6	−0.67	−0.66	0.6	0.59	1							
ΔH	0.97**	−0.96**	−0.58	−0.95*	0.96**	0.81	−0.96**	−0.91*	−0.61	1						
T_o	0.06	−0.01	0.52	0.03	0.05	−0.3	0	0.1	−0.19	0.25	1					
T_p	−0.98**	0.98**	0.74	0.94*	−0.98**	−0.93*	0.94*	0.91*	0.61	−0.92*	0.06	1				
T_e	−0.94*	0.96**	0.83	0.97**	−0.94*	−0.97**	0.96**	0.97**	0.53	−0.88*	0.23	0.96**	1			
Crys	0.99**	−0.98**	−0.64	−0.93*	0.99**	0.87	−0.94*	−0.90*	−0.65	0.97**	0.12	−0.98**	−0.91*	1		
SH	−0.98**	0.99**	0.72	0.98**	−0.97**	−0.91*	0.99**	0.97**	0.54	−0.96**	0.01	0.96**	0.97**	−0.96**	1	
DH	0.98**	−0.98**	−0.64	−0.94*	0.95*	0.86	−0.94*	−0.91*	−0.43	0.93*	−0.03	−0.96**	−0.95*	0.95*	−0.98**	1

[a] PV, peak viscosity; TV, trough viscosity; FV, final viscosity; PT, pasting temperature; ΔH, gelatinization enthalpy, T_o, onset gelatinization temperature; T_p, peak gelatinization temperature; T_e, end gelatinization temperature; Crys, crystallinity; SH, single helix; DH, double helix. *, significance difference at $p \leq 0.05$; **, significance difference at $p \leq 0.01$.

amount of mineral should promote greater charge−charge repulsion and increase the PV. The mineral content is highly correlated with the granule size, which is also correlated with the lipid, protein, and amylose content of the granule. The results suggest that the difference in the mineral contents of the fractions might not have a causal effect on PV as it is a minor component in the starch granules compared with lipid, protein, and starch.

PT showed a significant negative correlation ($R > -0.99$, $p < 0.01$) with granule size in MS, which is consistent with the higher lipid content in smaller MS granules (Table 1) inhibiting granule swelling to a greater extent as observed in the reduction of PV, resulting in a higher PT (Table 5). On the other hand, PT of PS fractions did not vary with granule size, which could be attributed to the smaller lipid contents of PS fractions compared with those of MS fractions (Table 1) and the high amount of phosphate groups in PS amylopectin (Table 2) promoting granule swelling, thus counteracting any inhibition effect of lipids.

In parallel with PV, the larger granules of MS had higher TV and FV than the smaller granules (Table 5). In contrast, the opposite trend was observed for PS fractions. This suggests that the exceptionally high PV of larger PS granule fractions caused the swollen granules to be more susceptible to shearing, thus displaying a lower TV than smaller granule fractions. In contrast, maize granules are less swollen (lower PV) and therefore less susceptible to shear-induced breakdown with consequent retention of the same order of viscosity in the TV and at the end of the test (FV) as at the peak (PV) (Figure 4; Table 5).

The increase in viscosity of starch paste during cooling has been associated with entanglement (retrogradation) of leached amylose.[49] FV increased significantly with increase in granule size of MS ($R \geq 0.99$, $p \leq 0.01$), which is in agreement with the amylose content of MS fractions (Table 1). The difference in FV of PS fractions was likely to be carried from the TV as the setback (FV-TV ~ 400) was similar for all fractions. It is often assumed that FV in pasting tests reflects molecular parameters, as most granule-level structuring is considered to have been lost. Although this argument could be made for MS, for which the larger granules with the higher amylose and lowest lipid contents have the higher FV, the opposite is true for PS. The smaller PS granules with high FV also had lower amylose contents, lower molecular size amylopectin, and higher levels of phosphorus, all factors that would be argued from a molecular perspective to generate lower FV values. The evidence from this study is that effects of granular features during the swelling phase dominate subsequent rheological properties during a pasting profile. This is analogous to the behavior of particles of gelling polysaccharides on hydration from an amorphous state,[50] in which properties are determined by a balance between hydration-driven swelling (as influenced here by, for example, phosphate substituents) and cross-linking within particles (as a major determinant of final viscosity). Similar considerations also apply to the stability of granule "ghosts",[51] the recoverable form of swollen granules.

Pearson's Correlation Matrix. The correlations among different parameters of MS and PS granule size fractions are presented in matrix form in Tables 6 and 7, respectively. As discussed above, the lipid contents in both starches showed a significant negative correlation with granule size; minerals in both starches tended to decrease with the increase in granule size; amylose showed the opposite trend (significant for PS, but not significant for MS). Compared with the protein and mineral contents, lipid contents showed a strong correlation with molecular structure and viscosity parameters in both starches. Similarly, gelatinization enthalpy was significantly correlated to single and double helices in both starches, whereas other gelatinization parameters (T_o, T_p, and T_c) showed mixed relationships with molecular structure. In conclusion, strong relationships were obtained linking granule size, lipid, supramolecular structure, and viscosity parameters in MS. Similarly, additional parameters such as amylose, ΔH, T_p, and T_c also showed strong correlations in PS, suggesting that chemical composition, supramolecular structure, pasting, and thermal properties are more closely related in PS fractions than in MS fractions; this might also be a reflection of the wider range of granule sizes in PS compared with MS.

Overall, the results show that the chemical composition of starch granules, such as lipid, protein, mineral, and apparent amylose contents, vary with granule size in both MS and PS. There is no obvious difference in amylose and amylopectin molecular structure in MS granules of different sizes. For PS, the hydrodynamic size of amylopectin and the amount of amylose increase with granule size, but the branch-chain length profiles of amylose and amylopectin do not vary. The smaller granules of both starches have lower crystallinity, suggesting that molecules closer to the hilum have more space constraint to align into crystallites than those closer to the surface, particularly for longer repeat distances within the B-type crystallites. The results have shown that it is possible to separate starch on the basis of granule size to produce fractions with more uniform and different structures and properties. Assuming that granule size reflects biosynthetic age, this study has demonstrated tight control of all glucan molecular parameters in MS as well as of branch length distributions in potato starch. In contrast, for PS, the relative amount of amylose and particularly the size of amylopectin molecules are shown to increase with granule size and presumed biosynthetic age.

AUTHOR INFORMATION

Corresponding Author

*Phone: (61) 7 33652145. Fax: (61) 7 33651177. E-mail: m.gidley@uq.edu.au.

Funding Sources

The University of Queensland Research Scholarship (UQRS), the University of Queensland International Research Award (UQIRA), and the Australian Research Council (Discovery Grant DP0985694) are acknowledged for funding this study.

ACKNOWLEDGMENT

We thank Drs. Bernadine Flanagan and Katia Strounina for their help in NMR analysis and interpretation.

REFERENCES

(1) Jane, J. L.; Kasemsuwan, T.; Leas, S.; Zobel, H.; Robyt, J. F. Anthology of starch granule morphology by scanning electron-microscopy. *Starch/Staerke* **1994**, *46*, 121–129.

(2) Ao, Z. H.; Jane, J. L. Characterization and modeling of the A- and B-granule starches of wheat, triticale, and barley. *Carbohydr. Polym.* **2007**, *67*, 46–55.

(3) Vasanthan, T.; Bhatty, R. S. Physicochemical properties of small- and large-granule starches of waxy, regular, and high-amylose barleys. *Cereal Chem.* **1996**, *73*, 199–207.

(4) Tang, H.; Ando, H.; Watanabe, K.; Takeda, Y.; Mitsunaga, T. Fine structures of amylose and amylopectin from large, medium, and small waxy barley starch granules. *Cereal Chem.* **2001**, *78*, 111–115.

(5) Chiotelli, E.; Le Meste, M. Effect of small and large wheat starch granules on thermomechanical behavior of starch. *Cereal Chem.* **2002**, *79*, 286–293.

(6) Soulaka, A. B.; Morrison, W. R. the amylose and lipid contents, dimensions, and gelatinization characteristics of some wheat starches and their A-granule and B-granule fractions. *J. Sci. Food Agric.* **1985**, *36*, 709–718.

(7) Takeda, Y.; Takeda, C.; Mizukami, H.; Hanashiro, I. Structures of large, medium and small starch granules of barley grain. *Carbohydr. Polym.* **1999**, *38*, 109–114.

(8) Pan, D. D.; Jane, J. L. Internal structure of normal maize starch granules revealed by chemical surface gelatinisation. *Biomacromolecules* **2000**, *1*, 126–132.

(9) Geddes, R.; Greenwood, C. T.; Mackenzie, S. Studies on the biosynthesis of starch granules. Part III: The properties of the componnet of staches from the growing potato tubers. *Carbohydr. Res.* **1965**, *1*, 71–82.

(10) Boyer, C. D.; Shannon, J. C.; Garwood, D. L.; Creech, R. G. Changes in starch granule size and amylose percentage during kernel development in several *Zea mays* L. genotypes. *Cereal Chem.* **1976**, *53*, 327–337.

(11) Evers, T.; Millar, S. Cereal grain structure and development: some implications for quality. *J. Cereal Sci.* **2002**, *36*, 261–284.

(12) Li, L.; Blanco, M.; Jane, J. L. Physicochemical properties of endosperm and pericarp starches during maize development. *Carbohydr. Polym.* **2007**, *67*, 630–639.

(13) Franco, C. M. L.; Ciacco, C. F. Factors that affect the enzymatic degradation of natural starch granules − effect of the size of the granules. *Starch/Staerke* **1992**, *44*, 422–426.

(14) Utrilla-Coello, R. G.; Agama-Acevedo, E.; de la Rosa, A. P. B.; Rodriguez-Ambriz, S. L.; Bello-Perez, L. A. Physicochemical and enzyme characterization of small and large starch granules isolated from two maize cultivars. *Cereal Chem.* **2010**, *87*, 50–56.

(15) Noda, T.; Takigawa, S.; Matsuura-Endo, C.; Kim, S. J.; Hashimoto, N.; Yamauchi, H.; Hanashiro, I.; Takeda, Y. Physicochemical properties and amylopectin structures of large, small, and extremely small potato starch granules. *Carbohydr. Polym.* **2005**, *60*, 245–251.

(16) Chen, Z.; Schols, H. A.; Voragen, A. G. J. Starch granule size strongly determines starch noodle processing and noodle quality. *J. Food Sci.* **2003**, *68*, 1584–1589.

(17) Kaur, L.; Singh, J.; McCarthy, O. J.; Singh, H. Physico-chemical, rheological and structural properties of fractionated potato starches. *J. Food Eng.* **2007**, *82*, 383–394.

(18) Singh, N.; Kaur, L. Morphological, thermal, rheological and retrogradation properties of potato starch fractions varying in granule size. *J. Sci. Food Agric.* **2004**, *84*, 1241–1252.

(19) Dhital, S.; Shrestha, A. K.; Gidley, M. J. Relationship between granule size and in vitro digestibility of maize and potato starches. *Carbohydr. Polym.* **2010**, *82*, 480–488.

(20) Eerlingen, R. C.; Cillen, G.; Delcour, J. A. Enzyme-resistant starch. 4. Effect of endogenous lipids and added sodium dodecyl-sulfate on formation of resistant starch. *Cereal Chem.* **1994**, *71*, 170–177.

(21) Jung, S.; Rickert, D. A.; Deak, N. A.; Aldin, E. D.; Recknor, J.; Johnson, L. A.; Murphy, P. A. Comparison of Kjeldahl and Dumas methods for determining protein contents of soybean products. *J. Am. Oil Chem. Soc.* **2003**, *80*, 1169–1173.

(22) Hoover, R.; Ratnayake, W. Determination of total amylose content of starch. In *Handbook of Food Analytical Chemistry − Water, Protein, Enzymes, Lipids, and Carbohydrates*; Wrolstad, R. E., Acree, T. E., Decker, E. A., Penner, M. H., Reid, D. S., Schwartz, S. J., Shoemaker, C. F., Smith, D., Sporns, P., Eds.; Wiley-Interscience: Hoboken, NJ, 2005; pp 689−691.

(23) American Association of Cereal Chemists. Ash-basic method 08-01 0.01. In *Approved Methods of the AACC*, 10th ed.; American Association of Cereal Chemists: St. Paul, MN, 2000.

(24) Cave, R. A.; Seabrook, S. A.; Gidley, M. J.; Gilbert, R. G. Characterization of starch by size-exclusion chromatography: the limitations imposed by shear scission. *Biomacromolecules* **2009**, *10*, 2245–2253.

(25) Dhital, S.; Shrestha, A. K.; Flanagan, B. M.; Hasjim, J.; Gidley, M. J. Cryo-milling of starch granules leads to differentail effects on molecular size and conformation. *Carbohydr. Polym.* **2011**, *84*, 1133–1140.

(26) Tizzotti, M. J.; Sweedman, M. C.; Tang, D.; Gilbert, R. G. New ^{1}H NMR procedure for the characterization of native and modified food-grade starches. *J. Agric. Food Chem.* **2011**, *59*, 6913–6919.

(27) Htoon, A.; Shrestha, A. K.; Flanagan, B. M.; Lopez-Rubio, A.; Bird, A. R.; Gilbert, E. P.; Gidley, M. J. Effects of processing high amylose

maize starches under controlled conditions on structural organisation and amylase digestibility. *Carbohydr. Polym.* **2009**, *75*, 236–245.

(28) Tan, I.; Flanagan, B. M.; Halley, P. J.; Whittaker, A. K.; Gidley, M. J. A method for estimating the nature and relative proportions of amorphous, single, and double-helical components in starch granules by C-13 CP/MAS NMR. *Biomacromolecules* **2007**, *8*, 885–891.

(29) Dhital, S.; Shrestha, A. K.; Gidley, M. J. Effect of cryo-milling on starches: functionality and digestibility. *Food Hydrocolloids* **2010**, *24*, 152–163.

(30) Swinkels, J. J. M. Composition and properties of commercial native starches. *Starch/Staerke* **1985**, *37*, 1–5.

(31) Galliard, T.; Bowler, P. Morphology and composition of starch. In *Starch: Properties and Potential*; Galliard, T., Ed.; Wiley: New York, 1987; pp 55−78.

(32) Morrison, W. R. Starch lipids − a reappraisal. *Starch/Staerke* **1981**, *33*, 408–410.

(33) Morrison, W. R. Lipids in cereal starches − a review. *Cereal Sci.* **1988**, *8*, 1–15.

(34) Hizukuri, S.; Tabata, S.; Nikuni, Z. Studies on starch phosphate. 1. Estimation of glucose-6-phosphate residues in starch and presence of other bound phosphate(s). *Starch/Staerke* **1970**, *22*, 338–343.

(35) Baldwin, P. M.; Melia, C. D.; Davies, M. C. The surface chemistry of starch granules studied by time-of-flight secondary ion mass spectrometry. *J. Cereal Sci.* **1997**, *26*, 329–346.

(36) Baldwin, P. M. Starch granule-associated proteins and polypeptides: a review. *Starch/Staerke* **2001**, *53*, 475–503.

(37) Raeker, M. O.; Gaines, C. S.; Finney, P. L.; Donelson, T. Granule size distribution and chemical composition of starches from 12 soft wheat cultivars. *Cereal Chem.* **1998**, *75*, 721–728.

(38) Jane, J. L.; Shen, J. J. Internal structure of the potato starch granule revealed by chemical gelatinization. *Carbohydr. Res.* **1993**, *247*, 279–290.

(39) Kossmann, J.; Lloyd, J. Understanding and influencing starch biochemistry. *Crit. Rev. Biochem. Mol. Biol.* **2000**, *35*, 41–196.

(40) Hasjim, J.; Lavau, G. C.; Gidley, M. J.; Gilbert, R. G. In vivo and in vitro starch digestion: are current in vitro techniques adequate?. *Biomacromolecules* **2010**, *11*, 3600–3608.

(41) Zobel, H. F. X-ray analysis of starch granules. In *Methods in Carbohydrate Chemistry − IV*; Whistler, R. L., Smith, R. J., BeMiller, J. N., Eds.; Academic Press: New York, 1964; pp 109−113.

(42) Franco, C. M. L.; Ciacco, C. F.; Tavares, D. Q. The structure of waxy corn starch: effect of granule size. *Starch/Staerke* **1998**, *50*, 193–198.

(43) Cooke, D.; Gidley, M. J. Loss of crystalline and molecular order during starch gelatinization − origin of the enthalpic transition. *Carbohydr. Res.* **1992**, *227*, 103–112.

(44) Vermeylen, R.; Goderis, B.; Reynaers, H.; Delcour, J. A. Gelatinisation related structural aspects of small and large wheat starch granules. *Carbohydr. Polym.* **2005**, *62*, 170–181.

(45) Waramboi, J. G.; Dennien, S.; Gidley, M. J.; Sopade, P. A. Characterisation of sweet potato from Papua New Guinea and Australia: Physicochemical, pasting and gelatinisation properties. *Food Chem.* **2011**, *26*, 1759–1770.

(46) Debet, M. R.; Gidley, M. J. Three classes of starch granule swelling: Iinfluence of surface proteins and lipids. *Carbohydr. Polym.* **2006**, *64*, 452–465.

(47) Tester, R. F.; Morrison, W. R. Swelling and gelatinization of cereal starches. 1. Effects of amylopectin, amylose, and lipids. *Cereal Chem.* **1990**, *67*, 551–557.

(48) Kasemwong, K.; Piyachomkwan, K.; Wansuksri, R.; Sriroth, K. granule sizes of canna (*Canna edulis*) starches and their reactivity toward hydration, enzyme hydrolysis and chemical substitution. *Starch/Staerke* **2008**, *60*, 624–633.

(49) Batey, I. L. Interpretation of RVA curves. In *The RVA Handbook*; Crosbie, G. B., Ross, A. S., Eds.; AOAC International: St. Paul, 2007; pp 19−29.

(50) Burey, P.; Bhandari, B. R.; Howes, T.; Gidley, M. J. Gel particles from spray-dried disordered polysaccharides. *Carbohydr. Polym.* **2009**, *76*, 206–213.

(51) Debet, M.; Gidley, M. J. Why do gelatinized starch granules not dissolve completely? Roles for amylose, protein, and lipid in granule "Ghost" integrity. *J. Agric. Food Chem.* **2007**, *55*, 4752–4760.